

Electrical Read-Out of a Single Spin Using an Exchange-Coupled Quantum Dot

Clément Godfrin,^{†,‡} Stefan Thiele,^{†,‡} Abdelkarim Ferhat,^{†,‡} Svetlana Klyatskaya,[¶] Mario Ruben,^{¶,§,||} Wolfgang Wernsdorfer,^{¶,†,‡} and Franck Balestro^{*,†,‡,||}

[†]CNRS Institut NEEL, Grenoble, F-38000, France

[‡]Université Grenoble Alpes, Institut NEEL, Grenoble, F-38000, France

[¶]Institute of Nanotechnology (INT) Karlsruhe Institute of Technology (KIT), 76344, Eggenstein-Leopoldshafen, Germany

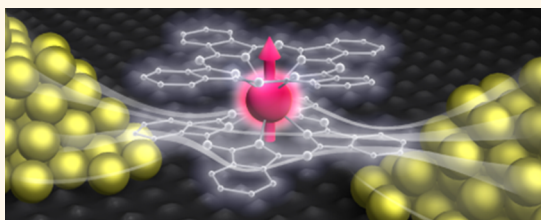
[§]Institut de Physique et Chimie des Matériaux de Strasbourg (IPCMS), CNRS-Université de Strasbourg, 67034, Strasbourg, France

^{||}Institut Université de France, 103 Boulevard Saint-Michel, 75005, Paris, France

Supporting Information

ABSTRACT: We present an original way of continuously reading-out the state of a single electronic spin. Our detection scheme is based on an exchange interaction between the electronic spin and a nearby read-out quantum dot. The coupling between the two systems results in a spin-dependent conductance through the read-out dot and establishes an all electrical and nondestructive single spin detection. With conductance variations up to 4% and read-out fidelities greater than 99.5%, this method represents an alternative to systems for which spin-to-charge conversion cannot be implemented. Using a semiclassical approach, we present an asymmetric exchange coupling model in good agreement with our experimental results.

KEYWORDS: quantum dot, single-molecule magnets, nanospintronic, single-molecule transistor, single-spin detection



Over the last 10 years, advances in nanofabrication and measurement technologies allowed for the read-out^{1–4} and manipulation^{5–11} of single electronic and nuclear spins. Besides the opportunity of testing our understanding of quantum mechanics, these progresses are at the heart of recent developments toward potential applications in the field of nanospintronics,^{12,13} molecular spintronics^{14–16,30} and quantum information processing.¹⁷ Among different concepts, systems integrating an all electrical spin detection benefit most from achievements of the microelectronic industry, but so far, they relied on the spin to charge conversion^{2,18,19} which required emptying the electron into a nearby reservoir. However, in devices where the energy of the spin system is much more negative than the Fermi energy of the leads, a different detection technique is mandatory. Here we present a general detection scheme based on the exchange coupling between a single electronic spin coupled to a read-out quantum dot. Depending on the strength of the exchange coupling, this detection scheme allows an all electrical and non destructive read-out of a single electronic spin, as the conductance of the read-out quantum dot is spin dependent.

To implement this general detection scheme, we made use of the electromigration technique²⁰ to fabricate a single TbPc₂ molecule spin-transistor (Figure 1a), that can be considered as two coupled quantum systems:

(i) First, an **electronic spin** carried by the terbium Tb³⁺ ion. Its total spin $S = 3$ and total orbital momentum $L = 3$ originate from its [Xe]4f⁸ electronic configuration. A strong spin–orbit coupling leads to a total angular magnetic moment $J = 6$ of the electronic spin. Moreover, the two phthalocyanines (Pc) generate a ligand field, leading an electron-spin ground state doublet $|\uparrow\rangle$ and $|\downarrow\rangle$. It results in an electronic-spin exhibiting a strong uniaxial anisotropy axis perpendicular to the plane defined by the phthalocyanines,²¹ as depicted in Figure 1a. At finite magnetic fields, the degeneracy of the doublet is lifted, the electronic spin can undergo a reversal by emitting a phonon *via* a direct relaxation process.

(ii) Second, the Pc ligands create a **read-out quantum dot**. The TbPc₂ has a spin $S = 1/2$ delocalized over the two Pc ligands²³ which is close in energy to the Tb-4f states. Thus, the delocalized π -electron system results in a quantum dot in the vicinity of the electronic spin carried by the Tb³⁺ ion. This read-out quantum dot is tunnel-coupled to source and drain terminals to perform transport measurements. As demonstrated in the following, a strong exchange interaction in between the delocalized π -electron and the Tb³⁺ **electronic spin** can be

Received: January 20, 2017

Accepted: April 11, 2017

Published: April 11, 2017

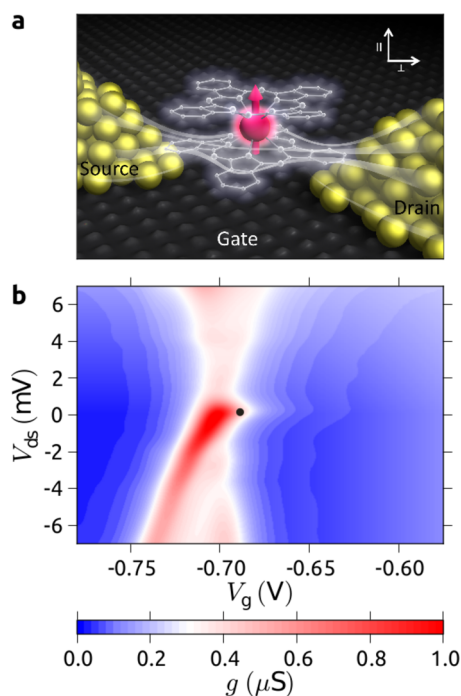


Figure 1. (a) Artist view of the three terminals TbPc₂ spin-transistor. It represents the one nanometer high TbPc₂ molecular magnet, contacted to the source and drain gold electrodes (yellow) and a back gate (not shown). The electronic spin of the Tb³⁺ ion (pink) is coupled to the Pc ligands read-out quantum dot (white) via exchange interaction. White lines represent electrons flow through the Pc read-out dot. This coupling modifies the chemical potential of the read-out quantum dot depending on the electronic spin state. As a result, the differential conductance is spin dependent. The orientation of the electronic spin also indicates the easy axis of the TbPc₂ molecular magnet. (b) Stability diagram of the read-out quantum dot showing the differential conductance as a function of the source-drain voltage V_{ds} and the back gate voltage V_g . The Kondo peak on the right side of the Coulomb diamond indicates an odd number of electrons into the read-out quantum dot. Measurements of Figure 2 are performed at the working point indicated by a black dot at $V_g = -0.69$ V and $V_{ds} = 0$ V.

observed, resulting in an electrical read-out of a single electronic spin without affecting its magnetic properties.

RESULTS

Now, we present the characterization of our single-molecule spin transistor measuring the differential conductance as a function of the source drain voltage V_{ds} and the gate voltage V_g at an electronic temperature around 80 mK to obtain the stability diagram presented in Figure 1b. Regions colored in red and blue exhibited respectively high and low differential conductance values. Note that this sample is the same as previously studied,^{4,22} the difference in conductance originating from a slight change of the molecules tunnel-coupling to the metallic leads due to aging of the device. From the general characteristics of the Coulomb diamond in Figure 1b, we obtained a conversion factor $\alpha = \Delta V_{ds}/\Delta V_g \approx 1/8$, resulting in a low estimation of the charging energy $E_C \approx 100$ meV of the quantum dot under investigation. First, this large value agrees with the idea depicted in Figure 1a that the single TbPc₂ molecular magnet can be the quantum dot under investigation. Moreover, it was proved by Zhu *et al.*²⁴ that electrons added to

the TbPc₂ preferentially go to the Pc ligands up to the fifth reduction and second oxidation. Thus, as observed in our previous works on two different samples,^{4,11,22} the charge state as well as the magnetic properties of the Tb³⁺ ion are conserved. On these complementary accounts, the read-out quantum dot is most likely created by the Pc ligands.

The stability diagram presented in Figure 1b exhibits a zero bias anomaly on the right side of the charge degeneracy point, which is associated with the usual spin $S = 1/2$ Kondo effect observed in 2D electron gas quantum dots^{25,26} and single molecule transistors.^{28,29} The Kondo temperature T_K was determined by measuring the differential conductance at $V_{ds} = 0$ V as a function of the temperature T for a fixed gate voltage

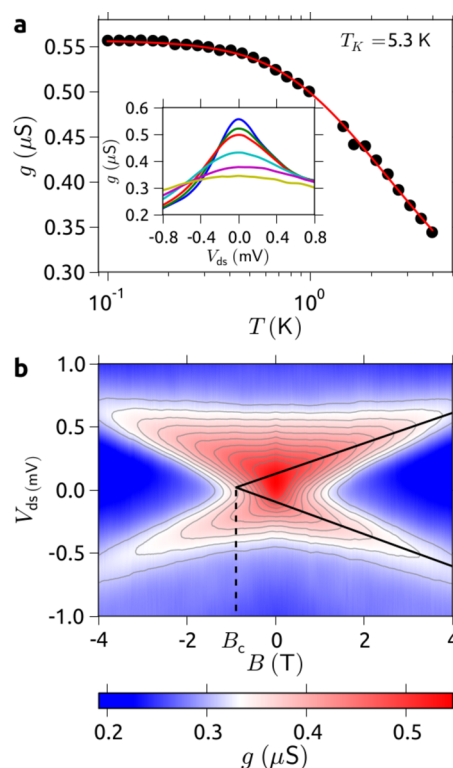


Figure 2. (a) Temperature dependence of the differential conductance $\delta I/\delta V$ at $V_{ds} = 0$ V. Inset: Evolution of $\delta I/\delta V$ versus V_{ds} for a different set of temperatures. The temperatures from highest to lowest conductance were 0.1 K, 0.7 K, 1 K, 2 K, 3 K, and 4.2 K. (b) Differential conductance as a function of the magnetic field B and the source-drain voltage V_{ds} . The solid lines were fitted to the maxima and extrapolated to negative magnetic fields. It indicates that the quantum dot under investigations possess a spin $S = 1/2$ and a g -factor $g = 2.15 \pm 0.1$. The critical field, given by the intersection of the two lines, was determined as $B_c = -0.88$ T, indicating a strong ferromagnetic coupling $a = -3.91$ T between the read-out quantum dot and the terbium spin.

$V_g = -0.69$ V (Figure 2a). By fitting the results to the empirical formula:²⁵

$$g(T) = g_0 \left(\frac{T^2}{T_K^2} (2^{1/s} - 1) + 1 \right)^{-s} + g_c \quad (1)$$

where g_0 is the maximum conductance, $s = 0.22$, and g_c is the fixed background conductance; we obtained a Kondo temperature $T_K = 5.3 \pm 0.05$ K.

To determine the configuration and value of the exchange coupling between the electronic spin and the read-out quantum dot carried by the Tb^{3+} ion, we investigated the evolution of the Kondo peak depending on the applied bias voltage V_{ds} and the external magnetic field B . By increasing B , the zero bias anomaly splits linearly, the value of the slope being $124 \mu\text{V}/\text{T}$, as presented in Figure 2b. This slope is a direct measurement of the g -factor $= 2.15 \pm 0.1$, which is consistent with the usual spin $S = 1/2$ Kondo effect.

For a standard spin $S = 1/2$ Kondo effect, an extrapolation of this linear splitting should give an intersection at a positive value of magnetic field B_c , where B_c is the critical magnetic field, and is a direct measurement of the Kondo temperature T_K via $2g\mu_B B_c = k_B T_K$. From the measurement presented in Figure 2b, we clearly observe a different behavior. An extrapolation results in a negative critical magnetic field $B_c \approx -880$ mT. To understand this behavior, we use the analogy to the underscreened spin $S = 1$ Kondo effect^{27,31} for which the Kondo resonance separates into Zeeman states for $2g\mu_B B_c \ll k_B T_K$. This effect originates from the ferromagnetic coupling of the remaining unscreened spin $S = 1/2$, reducing the strength of the antiferromagnetic coupling between the screened spin $S = 1/2$ and the electrons of the leads. Acting as an additional effective magnetic field, this ferromagnetic coupling lowers the value of B_c .

In our single molecular magnet spin-based transistor, the Tb^{3+} ion carries an electronic spin with a magnetic moment equal to $9 \mu_B$. The negative value of B_c originates from the ferromagnetic coupling between the read-out quantum dot and this electronic spin. Taking into account this coupling, the relation between the critical field B_c and the Kondo temperature T_K can be modified to⁴

$$2g\mu_B B_c = k_B T_K + a\mu_B J_z S_z \quad (2)$$

where a is the coupling constant, J_z and S_z are the z component of the electronic Tb^{3+} and read-out quantum dot spins, respectively. Using the Kondo temperature $T_K = 5.3$ K obtained from eq 1 and the critical field extracted from the magnetic field dependence (Figure 2b), a coupling constant $a = -3.91$ T is obtained. We emphasize that such a high value cannot be explained by a purely dipolar interaction due to the terbium magnetic moment. Indeed, the relative distance between the phthalocyanine read-out quantum dot and the Tb^{3+} ion is about 0.5 nm, giving a dipolar interaction of the order of 0.1 T, which is more than 1 order of magnitude lower than the measured coupling constant. As an efficient exchange interaction requires an overlap of the wave functions between the electronic magnetic moment carried by the Tb^{3+} ion and the read-out quantum dot, this high coupling further validates the expected configuration for which the read-out quantum dot is the phthalocyanine. We present in the Supporting Information two other TbPc_2 -based spin transistors for which the exchange coupling was measured.

We now present the measurements and the model to explain how the exchange coupling between the electronic spin state and the read-out quantum dot induces a spin dependence of the differential conductance. We first define B_{\parallel} and B_{\perp} being the magnetic fields applied parallel and perpendicular to the easy axis of the molecule, respectively (Figure 1a). For $V_{\text{ds}} = 0$ and $B_{\perp} = 0$, we recorded the differential conductance at the working point while sweeping B_{\parallel} (Figure 3a). By repeating this measurement, we obtained two distinct magneto-conductance signals, corresponding to the two electronic spin states $|\uparrow\rangle$

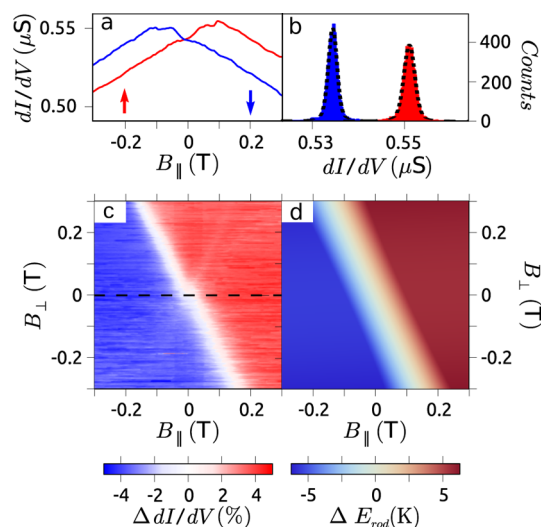


Figure 3. (a) Differential conductance of the read-out quantum dot at $V_{\text{ds}} = 0$ V as a function of the magnetic field B_{\parallel} with $B_{\perp} = 0$. The exchange coupling between the read-out quantum dot and the electronic spin results in two different conductance signals for the two spin orientations \uparrow (red) and \downarrow (blue). (b) Histogram of differential conductance values at $B_{\parallel} = +100$ mT for 10000 sweeps, showing two Gaussian-like distributions. From the overlap of the distributions we estimated a read-out fidelity of 99.5%. (c) Conductance difference between the spin up and down as a function of the magnetic field parallel (B_{\parallel}) and perpendicular (B_{\perp}) to the easy axis of the molecule. The dotted line corresponds to the configuration of panel a. (d) Calculated energy difference $\Delta E_{\text{rod}} = E_{\text{rod}}^{\uparrow} - E_{\text{rod}}^{\downarrow}$ within the read-out quantum dot as a function of the magnetic field B_{\parallel} and B_{\perp} .

(red) and $|\downarrow\rangle$ (blue). The two measurements intersect at $B_{\parallel} = 0$ and have a constant differential conductance difference for $B_{\parallel} > \pm 100$ mT. To quantify the read-out fidelity of our device, we recorded the conductance values at $B_{\parallel} = 100$ mT for 10000 measurements. Plotting the results into a histogram yielded two distinct Gaussian-like distributions as presented in Figure 3b. The read-out fidelity was determined to be higher than 99.5% by relating the overlap of the best fits to these two distributions.

To further characterize the signal originating from the electronic spin, we determined the conductance difference between the two different orientations of the electronic spin ($|\uparrow\rangle$ and $|\downarrow\rangle$) as a function of B_{\parallel} and B_{\perp} (Figure 3c). Two different regions are clearly visible. In the red region, the conductance corresponding to spin $|\downarrow\rangle$ is lower than that for spin $|\uparrow\rangle$. In the blue region, we observe the inverse scenario. However, at a particular combination of B_{\parallel} and B_{\perp} the signal goes to zero, which is indicated by the white region. The dotted line in Figure 3c emphasizes the cross-section presented in Figure 3a.

DISCUSSION

We now turn to the theoretical explanation of the magneto-conductance evolution as a function of B_{\parallel} and B_{\perp} . We use a semiclassical approach to describe the influence of the electronic spin J on the chemical energy of the read-out quantum dot. Our model takes into account the spin s of the read-out quantum dot, the Ising spin J of the Tb^{3+} 4f electrons, considering that both spins are subjected to an external magnetic field \mathbf{B} , and coupled through the exchange interaction. The Hamiltonian \mathcal{H} of the system is then given by

$$\begin{aligned}\mathcal{H} &= \mathcal{H}_J + \mathcal{H}_s + \mathcal{H}_{J,s} \\ &= \mathcal{H}_J + \mathcal{H}_{\text{rod}} \\ &= \mu_B \mathbf{B} \cdot g_J \mathbf{J} + \mu_B \mathbf{B} \cdot \bar{g}_s \cdot \mathbf{s} + \mathbf{J} \cdot \bar{a} \cdot \mathbf{s}\end{aligned}$$

where \bar{g}_s and g_J , respectively are the g -factor of the read-out quantum dot and of the electronic spin, \bar{a} is the exchange coupling, and μ_B is the Bohr magneton. In the experiment, the magnetic field \mathbf{B} is applied along two directions, such that it can be defined in the x - z plane of the TbPc₂ molecular magnet, resulting in $\mathbf{B} = (B_{\perp}, 0, B_{\parallel})$. Furthermore, $\mathbf{J} = \pm 6e_z$ is considered as a classical vector confined on the easy axis of the TbPc₂ molecular magnet.²¹ Because of the axial symmetry of the system, we consider it as invariant under a rotation in the x - y plan. The read-out dot Hamiltonian can be consequently defined in the (\perp , \parallel) basis as

$$\mathcal{H}_{\text{rod}} = \mu_B \begin{pmatrix} B_{\perp} \\ B_{\parallel} \end{pmatrix} \cdot \bar{g}_s \cdot \begin{pmatrix} s_{\perp} \\ s_{\parallel} \end{pmatrix} + \begin{pmatrix} J_{\perp} \\ J_{\parallel} \end{pmatrix} \cdot \bar{a} \cdot \begin{pmatrix} s_{\perp} \\ s_{\parallel} \end{pmatrix} \quad (3)$$

Because the spin \mathbf{s} of the read-out quantum dot can not be considered as a punctual electronic momentum aligned along the easy axis of terbium magnetization, the exchange interaction cannot be described by a diagonal tensor. Indeed the delocalization of the electron in the ligand involves a multipolar correction expressed in terms of coupling between the various spacial components, that is, off-diagonal terms in the exchange tensor \bar{a} . Moreover, the g -tensor is sensitive to the shape of the QD,³² and measurements^{33,34} in quantum dot showed a significant anisotropy of the g -factor which turned out to be tunable by electrical means.^{34,35} Therefore, due to the nonsymmetric coupling of the read-out quantum dot to the leads, and because no chemical environment argument can ensure an isotropic g -factor, the more general way to express the exchange tensor \bar{a} and the g -factor in the (\perp , \parallel) basis is

$$\bar{a} = \begin{pmatrix} a & \delta a_{\parallel} \\ \delta a_{\parallel} & a \end{pmatrix} \quad \bar{g}_s = \begin{pmatrix} g_s + \delta g_s & 0 \\ 0 & g_s \end{pmatrix} \quad (4)$$

where the notation “ δ ” is used for the anisotropic contributions. Subsequently, taking $s_{\perp} = \hbar\sigma_x/2$ and $s_{\parallel} = \hbar\sigma_z/2$, the Hamiltonian \mathcal{H}_{rod} in the read-out dot electronic spin basis is given by

$$\begin{aligned}\mathcal{H}_{\text{rod}} &= \frac{\hbar\mu_B g_s B_{\parallel}}{2} \begin{pmatrix} 1 & \left(1 + \frac{\delta g_s}{g_s}\right) \frac{B_{\perp}}{B_{\parallel}} \\ \left(1 + \frac{\delta g_s}{g_s}\right) \frac{B_{\perp}}{B_{\parallel}} & -1 \end{pmatrix} \\ &+ \frac{\hbar a J_z}{2} \begin{pmatrix} 1 & \frac{\delta a_{\parallel}}{a} \\ \frac{\delta a_{\parallel}}{a} & -1 \end{pmatrix}\end{aligned} \quad (5)$$

The eigenenergies of the read-out dot are

$$E_{s=\pm 1/2} = \pm [\epsilon_0 + 2ag_s\mu_B B_{\parallel} J_z + 2\delta a(g_s + \delta g_s)\mu_B B_{\parallel} J_z]^{1/2} \quad (6)$$

where ϵ_0 is function of J_z^2 , meaning that the states $J_z = \pm 6$ are degenerated for $ag_s B_{\parallel} = -\delta a(g_s + \delta g_s)B_{\perp}$. This results in a shift of the crossing point in B_{\parallel} as the function of B_{\perp} observed in the measurement presented in Figure 3c, given by

$$B_{\parallel}^{\text{shift}} = \frac{(g_s + \delta g_s)}{g_s} \frac{\delta a_{\parallel}}{a} B_{\perp} \quad (7)$$

To obtain an estimation of the off-diagonal term δa_{\parallel} , as well as the anisotropy of g_s , we use the experimental values determined from the measurements presented in Figure 2 ($a = -3.91$ T and $g \approx 2.15$), and extract the slope of $B_{\parallel}^{\text{shift}} = -0.6B_{\perp}$ from the measurement presented in Figure 3c. We calculated and present in Figure 4 the different doublet $\left(\frac{\delta g_s}{g_s}; \frac{\delta a_{\parallel}}{a}\right)$ in

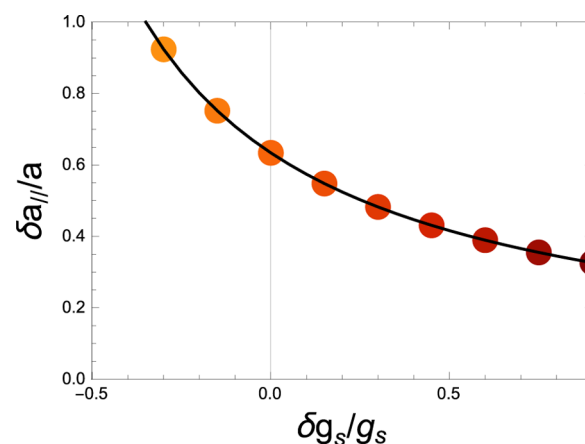


Figure 4. Fitting parameter line as a function of $\left(\frac{\delta g_s}{g_s}; \frac{\delta a_{\parallel}}{a}\right)$.

accordance with the experimental measurements. An infinite number of doublets gives a perfect agreement with the experiment. Minimizing the anisotropy of the g -factor, we use $\left(\frac{\delta g_s}{g_s} = 0; \frac{\delta a_{\parallel}}{a} = 0.6\right)$, we obtain the energy difference of the read-out quantum dot: $\Delta E_{\text{rod}} = E_{\text{rod}}^{\uparrow} - E_{\text{rod}}^{\downarrow}$ depending on the state $|\uparrow\rangle$ or $|\downarrow\rangle$ of the electronic spin, as a function of B_{\perp} and B_{\parallel} (Figure 3d). The zero sensitivity region (in white in Figure 3c) as well as the qualitative agreement reinforce the model used to interpret the dependence of the magneto-conductance signal as a function of the electronic spin orientation.

CONCLUSIONS

In summary, we report on the proposition, theoretical explanation, and experimental realization of an electrical read-out of a single electronic spin using an exchange coupled read-out quantum dot. This experimental realization has been demonstrated using the net magnetic moment of a single molecule, the read-out quantum dot being directly sensitive to the spin orientation resulting in signal amplitudes up to 4% and read-out fidelities of 99.5%. This detection scheme is fully consistent with any single molecule architecture for which the magnetic moment is carried by a single atom embedded by a ligand, as far as the charge state of the spin dot remains unchanged, as it is the case for all of the lanthanide double-decker family (Tb, Dy, Ho, etc.), and could also allow the detection of a single magnetic impurity in semiconductor quantum dots, or single spin coupled to a nanotube or

nanowire, leading to potential progress in nanospintronic and quantum information processing.

METHODS

The single TbPc₂ spin-based transistor was fabricated using an electromigration technique²⁰ at very low temperature. Using standard optical and e-beam lithography techniques, a gold nanowire on an Au/HfO₂ gate fabricated through atomic-layer deposition was prepared. After a cleaning procedure of the nanowire was performed with the use of acetone, ethanol, isopropyl alcohol solution, and oxygen plasma, a dilute dichloromethane solution of the TbPc₂ was deposited onto the nanowire at room temperature. The device was then connected on its sample holder, and enclosed in a high-frequency, low-temperature filter. It consists of 24 superconducting wires coated with Eccosorb, and enclosed in a CuNi tube of 1.5 mm external diameter. This filter is thermalized to the 40 mK stage of a dilution refrigerator resulting in an electronic temperature of about 50 mK. A nanogap was created in the nanowire ramping the voltage (10 mV/s) at 50 mK, and measuring its conductance using a fast feedback-loop (1.5 μs). Transport measurements on the single TbPc₂ spin-based transistor were performed at 40 mK in a dilution refrigerator equipped with a homemade three-dimensional vector magnet. It allows a sweep of the magnetic field in 3D at rates up to 0.2 T s⁻¹. A lock-in signal was generated by a 16 bits DA converter, and voltage was divided by 10³ to increase the signal-to-noise ratio. The read-out quantum dot signal was measured using a homemade room temperature I/V converter.

ASSOCIATED CONTENT

Supporting Information

The Supporting Information is available free of charge on the ACS Publications website at DOI: 10.1021/acsnano.7b00451.

Two other TbPc₂ spin-based transistors for which the exchange coupling was measured (PDF)

AUTHOR INFORMATION

Corresponding Author

*E-mail: franck.balestro@neel.cnrs.fr.

ORCID

Mario Ruben: 0000-0002-7718-7016

Franck Balestro: 0000-0001-7554-3841

Notes

The authors declare no competing financial interest.

ACKNOWLEDGMENTS

This work was partially supported by MoQuaS FP7-ICT-2013-10, the DFG Programs No. SPP 1459 and No. TRR 88 3Met, ANR-12-JS10-007 SINUSManip, ANR MolQuSpin. The samples were manufactured at the NANOFAB facilities of the Néel Institute. The authors thank E. Eyraud, Y. Deschanel, D. Lepoittevin, C. Hoarau, E. Bonet and C. Thirion, and are grateful to B. Canals for sharing his fruitful expertise about the nature of interactions in magnetic system

REFERENCES

- (1) Elzerman, J. M.; Hanson, R.; van Beveren, L. W.; Witkamp, B.; Vandersypen, L. M. K.; Kouwenhoven, L. P. Single-Shot Read-Out of an Individual Electron Spin in a Quantum Dot. *Nature* **2004**, *430*, 431–435.
- (2) Morello, A.; Pla, J. J.; Zwanenburg, F. A.; Chan, K. W.; Tan, K. Y.; Huebl, H.; Alves, A. D. Single-Shot Readout of an Electron Spin in Silicon. *Nature* **2010**, *467*, 687–691.
- (3) Neumann, P.; Beck, J.; Steiner, M.; Remp, F.; Fedder, H.; Hemmer, P. R.; Wrachtrup, J.; Jelezko, F. Single-Shot Readout of a Single Nuclear Spin. *Science* **2010**, *329*, 542–544.

- (4) Vincent, R.; Klyatskaya, S.; Ruben, M.; Wernsdorfer, W.; Balestro, F. Electronic Read-Out of a Single Nuclear Spin Using a Molecular Spin Transistor. *Nature* **2012**, *488*, 357–360.

- (5) Jelezko, F.; Gaebel, T.; Popa, I.; Gruber, A.; Wrachtrup, J. Observation of Coherent Oscillations in a Single Electron Spin. *Phys. Rev. Lett.* **2004**, *92*, 076401.

- (6) Koppens, F. H. L.; Buizert, C.; Tielrooij, K. J.; Vink, I. T.; Nowack, K. C.; Meunier, T.; Kouwenhoven, L. P.; Vandersypen, L. M. K. Driven Coherent Oscillations of a Single Electron Spin in a Quantum Dot. *Nature* **2006**, *442*, 766–771.

- (7) Pioro-Ladriere, M.; Obata, T.; Tokura, Y.; Shin, Y. S.; Kubo, T.; Yoshida, K.; Taniyama, T.; Tarucha, S. Electrically Driven Single-Electron Spin Resonance in a Slanting Zeeman Field. *Nat. Phys.* **2008**, *4*, 776–779.

- (8) Koehl, W. F.; Buckley, B. B.; Heremans, F. J.; Calusine, G.; Awschalom, D. D. Room Temperature Coherent Control of Defect Spin Qubits in Silicon Carbide. *Nature* **2011**, *479*, 84–87.

- (9) Pla, J. J.; Tan, K. Y.; Dehollain, J. P.; Lim, W. H.; Morton, J. J.; Jamieson, D. N.; Dzurak, A. S.; Morello, A. A Single-Atom Electron Spin Qubit in Silicon. *Nature* **2012**, *489*, 541–545.

- (10) Pla, J. J.; Tan, K. Y.; Dehollain, J. P.; Lim, W. H.; Morton, J. J.; Zwanenburg, F. A.; Jamieson, D. J.; Dzurak, A. S.; Morello, A. High-Fidelity Readout and Control of a Nuclear Spin Qubit in Silicon. *Nature* **2013**, *496*, 334–338.

- (11) Thiele, S.; Balestro, F.; Ballou, R.; Klyatskaya, S.; Ruben, M.; Wernsdorfer, W. Electrically Driven Nuclear Spin Resonance in Single-Molecule Magnets. *Science* **2014**, *344*, 1135–1138.

- (12) Wolf, S. A.; Awschalom, D. D.; Buhrman, R. A.; Daughton, J. M.; Von Molnar, S.; Roukes, M. L.; Chtchelkanova, A. Y.; Treger, D. M. Spintronics: a Spin-Based Electronics Vision for the Future. *Science* **2001**, *294*, 1488–1495.

- (13) Seneor, P.; Bernard-Mantel, A.; Petroff, F. Nanospintronics: When Spintronics Meets Single Electron Physics. *J. Phys.: Condens. Matter* **2007**, *19*, 165222.

- (14) Rocha, A. R.; Garcia-Suarez, V. M.; Bailey, S. W.; Lambert, C. J.; Ferrer, J.; Sanvito, S. Towards Molecular Spintronics. *Nat. Mater.* **2005**, *4*, 335–339.

- (15) Urdampilleta, M.; Klyatskaya, S.; Cleuziou, J.-P.; Ruben, M.; Wernsdorfer, W. Supramolecular Spin Valves. *Nat. Mater.* **2011**, *10*, 502–506.

- (16) Bogani, L.; Wernsdorfer, W. Molecular Spintronics Using Single-Molecule Magnets. *Nat. Mater.* **2008**, *7*, 179–186.

- (17) Loss, D.; DiVincenzo, D. P. Quantum Computation with Quantum Dots. *Phys. Rev. A: At., Mol., Opt. Phys.* **1998**, *57*, 120.

- (18) Field, M.; Smith, C. G.; Pepper, M.; Ritchie, D. A.; Frost, J. E. F.; Jones, G. A. C.; Hasko, D. G. Measurements of Coulomb Blockade with a Noninvasive Voltage Probe. *Phys. Rev. Lett.* **1993**, *70*, 1311.

- (19) Meded, V.; Bagrets, A.; Fink, K.; Chandrasekar, R.; Ruben, M.; Evers, F.; Bernard-Mantel, A.; Seldenthuis, J. S.; Beukman, A.; Van der Zant, H. S. J. Electrical Control over the Fe (II) Spin Crossover in a Single Molecule: Theory and Experiment. *Phys. Rev. B: Condens. Matter Mater. Phys.* **2011**, *83*, 245415.

- (20) Park, H.; Lim, A. K.; Alivisatos, A. P.; Park, J.; McEuen, P. L. Fabrication of Metallic Electrodes with Nanometer Separation by Electromigration. *Appl. Phys. Lett.* **1999**, *75*, 301–303.

- (21) Ishikawa, N.; Sugita, M.; Okubo, T.; Tanaka, N.; Iino, T.; Kaizu, Y. Determination of Ligand-Field Parameters and f-Electronic Structures of Double-Decker Bis(Phthalocyaninato)Lanthanide Complexes. *Inorg. Chem.* **2003**, *42*, 2440–2446.

- (22) Thiele, S. Read-Out and Coherent Manipulation of an Isolated Nuclear Spin. *Springer Theses* **2016**, 87.

- (23) Vitali, L.; Fabris, S.; Conte, A. M.; Brink, S.; Ruben, M.; Baroni, S.; Kern, K. Electronic Structure of Surface-Supported Bis(Phthalocyaninato)Terbium (III) Single Molecular Magnets. *Nano Lett.* **2008**, *8*, 3364–3368.

- (24) Zhu, P.; Lu, F.; Pan, N.; Arnold, D. P.; Zhang, S.; Jiang, J. Comparative Electrochemical Study of Unsubstituted and Substituted Bis(Phthalocyaninato) Rare Earth (III) Complexes. *Eur. J. Inorg. Chem.* **2004**, *2004*, 510–517.

- (25) Goldhaber-Gordon, D.; Shtrikman, H.; Mahalu, D.; Abusch-Magder, D.; Meirav, U.; Kastner, M. A. Kondo Effect in a Single-Electron Transistor. *Nature* **1998**, *391*, 156–159.
- (26) Cronenwett, S. M.; Oosterkamp, T. H.; Kouwenhoven, L. P. A Tunable Kondo Effect in Quantum Dots. *Science* **1998**, *281*, 540–544.
- (27) Nozières, Ph.; Blandin, A. Kondo Effect in Real Metals. *J. Phys. (Paris)* **1980**, *41*, 193.
- (28) Park, J.; Pasupathy, A. N.; Goldsmith, J. I.; Chang, C.; Yaish, Y.; Petta, J. R.; Rinkoski, M.; Sethna, J. P.; Abruña, H. D.; McEuen, P. L.; Ralph, D. C. Coulomb Blockade and the Kondo Effect in Single-Atom Transistors. *Nature* **2002**, *417*, 722–725.
- (29) Liang, W.; Shores, M. P.; Bockrath, M.; Long, J. R.; Park, H. Kondo Resonance in a Single-Molecule Transistor. *Nature* **2002**, *417*, 725–729.
- (30) Ganzhorn, M.; Klyatskaya, S.; Ruben, M.; Wernsdorfer, W. Strong Spin-Phonon Coupling Between a Single-Molecule Magnet and a Carbon Nanotube Nanoelectromechanical System. *Nat. Nanotechnol.* **2013**, *8*, 165–169.
- (31) Roch, N.; Florens, S.; Costi, T. A.; Wernsdorfer, W.; Balestro, F. Observation of the Underscreened Kondo Effect in a Molecular Transistor. *Phys. Rev. Lett.* **2009**, *103*, 197202.
- (32) Hanson, R.; Kouwenhoven, L. P.; Petta, J. R.; Tarucha, S.; Vandersypen, L. M. K. Spins in Few-Electron Quantum Dots. *Rev. Mod. Phys.* **2007**, *79*, 1217.
- (33) d'Hollosy, S.; Fábán, G.; Baumgartner, A.; Nygård, J.; Schönenberger, C. *g*-Factor Anisotropy in Nanowire-Based InAs Quantum Dots. *AIP Conf. Proc.* **2012**, 359.
- (34) Takahashi, S.; Deacon, R. S.; Oiwa, A.; Shibata, K.; Hirakawa, K.; Tarucha, S. Electrically Tunable Three-Dimensional *g*-Factor Anisotropy in Single InAs Self-Assembled Quantum Dots. *Phys. Rev. B: Condens. Matter Mater. Phys.* **2013**, *87*, 161302.
- (35) Deacon, R. S.; Kanai, Y.; Takahashi, S.; Oiwa, A.; Yoshida, K.; Shibata, K.; Hirakawa, K.; Tokura, Y.; Tarucha, S. Electrically Tuned *g* Tensor in an InAs Self-Assembled Quantum Dot. *Phys. Rev. B: Condens. Matter Mater. Phys.* **2013**, *84*, 041302.